Implementation of the Incremental Analysis Update (IAU) in ROMS 4D-Var

1. Introduction

Since no dynamical balance constraint is imposed on the analysis increments computed during 4D-Var, the resulting geostrophic adjustment process at the beginning of the assimilation window can lead to the generation of large amplitude inertia-gravity waves, so-called "initialization shocks." These waves typically dissipate within 12-24 hours and are not usually a concern for the physical circulations that develop at the end of the assimilation window. However, for coupled biogeochemical configurations of ROMS, or those that include sediment processes, these inertia-gravity waves can be very detrimental. Therefore, it is desirable to suppress the generation of inertia-gravity waves during the assimilation window to the maximum extent possible.

Initialization shock is a serious issue in numerical weather prediction (NWP), and mitigation attempts have a long history (e.g. Machenhaur,1977). Two common approaches used to minimize the influence of initialization shock in modern NWP systems are the application of a digital filter (Gauthier and Thépaut, 2001) and incremental analysis updates (IAU; Bloom *et al.*, 1996), although under certain conditions, the two approaches are equivalent (Polavarapu *et al.*, 2004). IAU is particularly easy to implement and has been included as an option in ROMS 4D-Var.

Following the usual convention, we will denote by $\boldsymbol{x}(t_k)$ the ocean state-vector at time t_k. Integration of the ROMS nonlinear model can then be represented as $\boldsymbol{x}(t_{k+1}) = \mathcal{M}(\boldsymbol{x}(t_k))$ where $\mathcal{M}$ represents the nonlinear model operators. Let $[t_k - \tau, t_k]$ represent the 4D-Var data assimilation window of length τ, where t_k is the current time. The usual practice in 4D-Var is to compute the analysis increment $\Delta\boldsymbol{x}(t_k - \tau)$ at the beginning of the analysis window, and then integrate $\boldsymbol{x}(t_k - \tau) + \Delta\boldsymbol{x}(t_k - \tau)$ forward in time to the end of the assimilation window using the nonlinear model $\mathcal{M}$. This occurs at the end of each 4D-Var outer-loop. However, since no explicit dynamical balance constraints are imposed on $\Delta\boldsymbol{x}(t_k - \tau)$, the ensuing geostrophic adjustment process during the assimilation window $[t_k - \tau, t_k]$ can lead to the generation of inertia-gravity waves as described above. Instead of adding the increment $\Delta\boldsymbol{x}(t_k - \tau)$ to the initial condition $\boldsymbol{x}(t_k - \tau)$, the IAU approach imposes the increment as a forcing term in the nonlinear model so that:

$$\boldsymbol{x}(t_{k+1}) = \mathcal{M}\big(\boldsymbol{x}(t_k)\big) + \boldsymbol{f}(t) \qquad (1)$$

where $\boldsymbol{f}(t) = \Delta\boldsymbol{x}(t_k - \tau)\Delta t/T$ for $t_k - \tau \le t \le t_k - \tau + T$ and $\boldsymbol{f}(t) = 0$ for $t > t_k - \tau + T$. In this way, the nonlinear model at the end of each outer-loop can be gently steered toward the desired analysis increment over some time interval $[t_k - \tau, t_k - \tau + T]$ during the assimilation window with the result that the initialization shock is greatly reduced. The size of the forcing term $\boldsymbol{f}(t)$ each timestep Δt depends on the choice of T, which in turn influences the filtering properties of the IAU procedure. The IAU procedure as implemented in ROMS is illustrated in Fig. 1. Since the forcing amplitude is generally small, the response function resulting from IAU can be conveniently quantified using the tangent linear approximation as described by Bloom *et al.* (1996). The connection of the IAU and the digital filter approach was explored by Polavarapu *et al.* (2004).

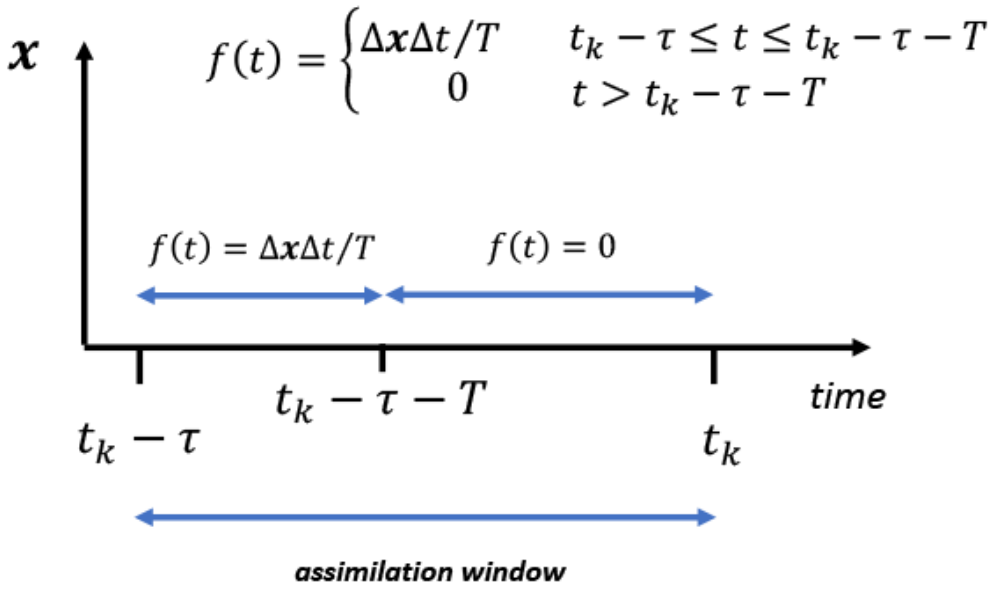

Figure 1: A schematic representation of the Incremental Analysis Update (IAU) as applied in ROMS.

2. ROMS Implementation

In ROMS 4D-Var, the IAU is activated by the parameter *timIAU* in *s4dvar.in*, where *timIAU* represents T in the equation for $\boldsymbol{f}(t)$ introduced in Section 1. If *timIAU*=0, then the IAU is not applied and the increment $\Delta \boldsymbol{x}(t_k - \tau)$ is added to the initial condition at the beginning of the analysis window as normal.

NOTE: The IAU is only available for dual 4D-Var using the *RBL4DVAR* and *SPLIT_RBL4DVAR* algorithms. IAU is not currently implemented in the primal formulation of 4D-Var (*I4DVAR*).

If *timIAU*$\neq 0$ then the IAU is activated in each outer-loop. If running *SPLIT_RBL4DVAR*, the *analysis* phase can be run separately with different values of *timIAU* but **ONLY** if *timIAU* was originally chosen to be non-zero in the *background* and *increment* phases. This allows users to explore different choices of *timIAU* without the need to rerun the inner-loops.

3. Examples

Application of the IAU in ROMS 4D-Var will be illustrated in two different configurations: the standard test case configured for the California Current system (WC13), and a triply nested configuration for the Mid-Atlantic Bight.

3.1 WC13

The first demonstration of the use of the IAU in ROMS uses the standard WC13 test case. This is a single 4D-Var cycle spanning 4-days (3-7 Jan, 2004) in which observations of SST, SSH and *in situ* profiles of temperature and salinity from Argo floats were assimilated. The dual formulation (*RBL4DVAR*) was used with 1 outer-loop and 25 inner-loops. Figure 2 (top panel) shows the inner-loop cost function resulting for the 25 inner-loops which is independent of the choice of time interval T over which the IAU is applied. Also shown in the top panel of Fig. 2 is the value of the cost function at the end of the outer-loop for several different choices of T in the range 0-4 days. The case $T = 0$ corresponds to the situation where the analysis increment $\Delta \boldsymbol{x}$ is added to the background initial condition at the beginning of the analysis window as normal. The case $T = 4$ days corresponds to applying IAU over the entire length of the assimilation window. For clarity, Fig. 2 (bottom panel) shows the outer-loop cost function versus T and shows that as T decreases, the cost function approaches the value when IAU is not applied, although in a non-monotonic manner. Interestingly, the smallest value of the cost function occurs when $T = 0.5$ days. Figure 3 shows the contribution of the different observation types to outer-loop cost function versus T and indicates that the non-monotonic behavior apparent in Fig. 2 is due mainly to the temperature observations.

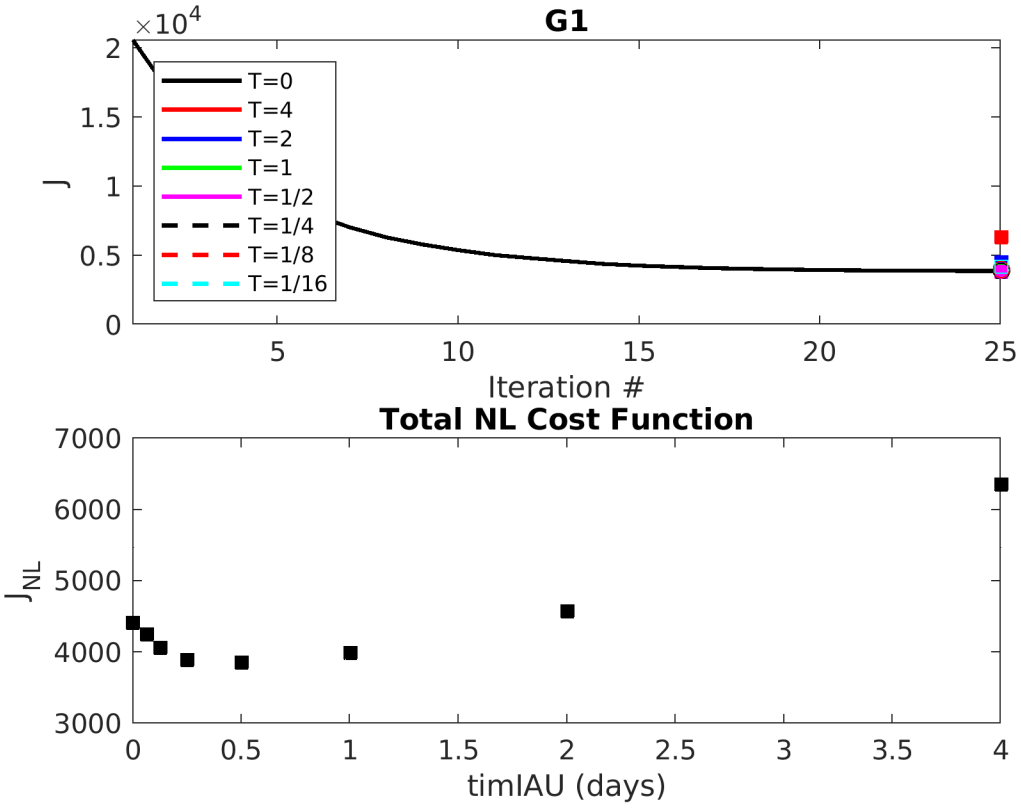

Figure 2: *Top panel*: The inner-loop cost function versus the number of inner-loops. The outer-loop cost function for different choices of *T* ranging from 0 (no IAU) to 4 days (the full length of the assimilation window) is also shown as the colored symbols. *Bottom panel*: The outer-loop cost function versus *T*. The case *T=0* corresponds to the usual

application of 4D-Var in which the analysis increment is added to the background at the beginning of the data assimilation window in the usual way.

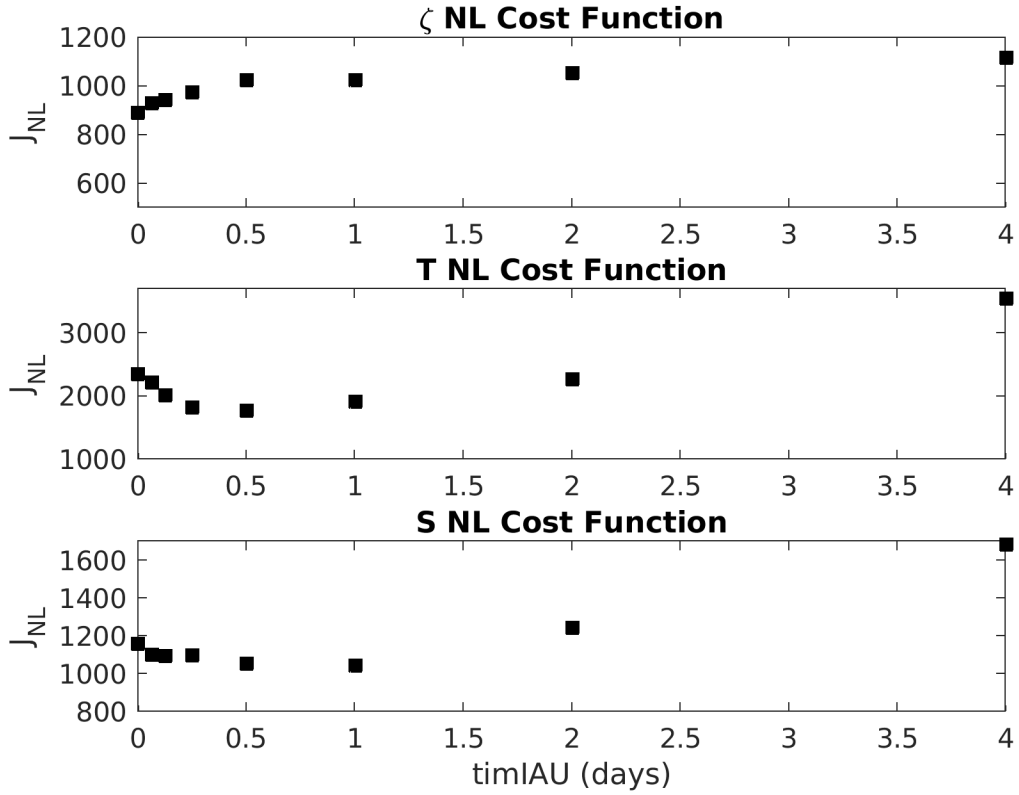

Figure 3: The contribution to the outer-loop cost function for the different observation types versus *T*. *top:* sea surface elevation, *middle:* temperature; *bottom:* salinity.

3.2 Nested 4D-Var

The second demonstration of the IAU is for a triply nested configuration of ROMS centered on the Mid-Atlantic Bight. The outer-most grid has a resolution ~7 km and is referred to as grid G1. The second and third nested grids are based on a horizontal refinement ratio of 3:1 and have resolutions ~2.3 km and ~0.8 km respectively. The second level nested grid is referred to as G2 while the inner-most grid is referred to as G3. The grid configuration is illustrated in Fig. 5a. Two-way nesting is employed across all of the grid boundaries.

In this application, the 4D-Var window has a duration of 3-days, and comprises 2 outer-loops and 7 inner-loops. Observations assimilated include satellite SST, along-track altimetry, *in situ* temperature, salinity and velocity, and gridded estimates of surface currents derived from HF radar.

The inner-loop cost function during each inner-loop versus the IAU interval *T* is shown in Fig. 4. The cost function is the same during the 1st outer-loop regardless of the value of *T*. The case

where no IAU is applied is represented by $T = 0$. During the 2nd inner-loop, the cost function increases with T as expected reflecting the reduction in the fit of the model to the observations at the end of the 1st outer-loop, although the rate of convergence of the inner-loop cost function is largely independent of T.

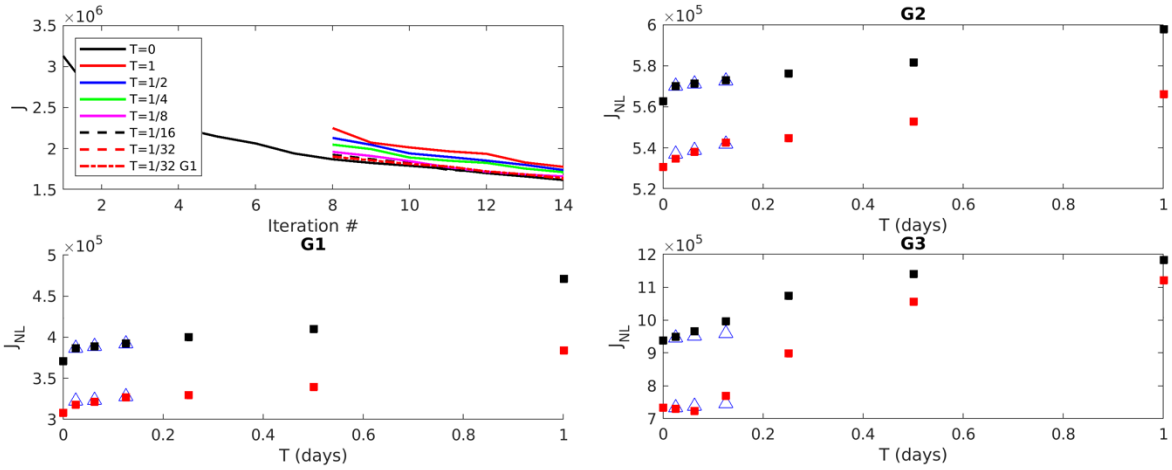

Figure 4: The inner-loop cost function for each outer-loop for different choices of T (upper left). The outer-loop cost function versus T for each grid for outer-loop 1 (black squares) and outer-loop 2 (red squares). The case when IAU is applied only on the G1 grid is represented by the blue open triangles.

The outer-loop cost function versus T for each outer-loop on each grid is also shown in Fig. 4. In general, as T decreases the outer-loop cost function approaches the case where no IAU is applied ($T = 0$), although as in the previous example, this is not always monotonic.

An illustration of the initialization shock that results when the IAU is not applied is shown in Figs. 5a-c which shows the sea surface elevation *increment* 1 hour after a 4D-Var initialization in the 2nd outer-loop when $T = 0$. The signature of gravity waves with amplitudes of up to 0.5 m is clearly evident in all three grids. The effectiveness of the IAU at reducing or mitigating the initialization shock is illustrated in Figs. 5d-i. Figures 5d and 5g show the sea surface elevation 6 hours after 4D-Var initialization when no IAU is applied for grids G1 and G2 respectively. The signatures of gravity waves on the shelf and in the vicinity of coastal features is very evident. Figures 5e and 4h show sea surface elevation when the IAU is applied over the first 6 hours of the assimilation window. Clearly the IAU is very effective at reducing the gravity wave shocks. However, as Fig. 4 reveals, the outer-loop cost function is larger than for the case $T = 0$, particularly on the inner-most grid G3. A closer fit to the observations can be achieved using a shorter IAU interval T. Figures 5f and 5i show the case when the IAU is applied over the first 1.5 hours of the assimilation window. In this more aggressive case, the outer-loop cost function is only a little higher than in the no IAU case (Fig. 4), although Figs. 5f and 5i show that some residual gravity wave signature is still present, though much reduced in amplitude compared to the no IAU case in Figs. 5d and 5g.

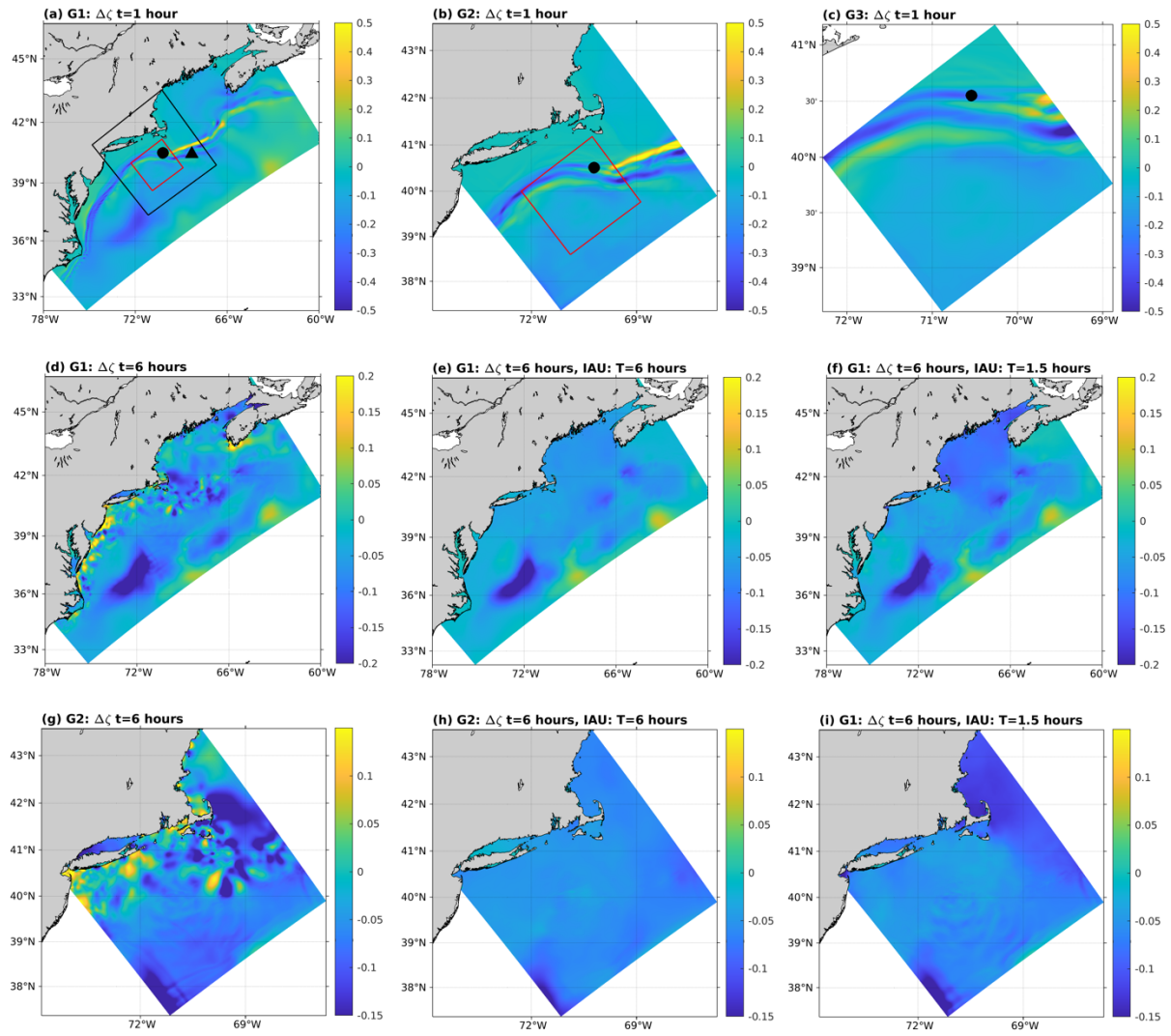

Figure 5: Sea surface elevation *increment* is shown 1 hour after a 4D-Var initialization in the 2nd outer-loop for the case when no IAU is used (*T=0*) for (a) G1, (b) G2 and (c) G3. The relative locations of the two-way nested grids are shown in (a) and (b). The black circle and triangle indicate the location of the time series shown in Figs. 5 and 6. The sea surface elevation after 6 hours for G1 is shown for (d) *T=0*, (e) *T=6* hours, and (f) *T=1.5* hours. Similarly, sea surface elevation after 6 hours for G2 is shown for (g) *T=0*, (h) *T=6* hours, and (i) *T=1.5* hours.

The temporal evolution of the sea surface elevation *increment* is shown in Figs. 6 and 7 in the form of time series at the locations indicated in Fig. 5a. The large amplitude gravity waves resulting from the initialization shock when no IAU is applied are very evident. Figures 6 and 7 reveal that applying the IAU over an interval 1.5 hours or longer is very effective at eliminating the gravity wave signature. As noted above though, this comes at the cost of reducing the fit of the model to the observations. While the more aggressive approach of applying the IAU over shorter intervals than 1.5 hours produces a closer fit to the observations (Fig. 4), some gravity wave signatures are still present as shown in Figs. 6 and 7, albeit with a reduced amplitude.

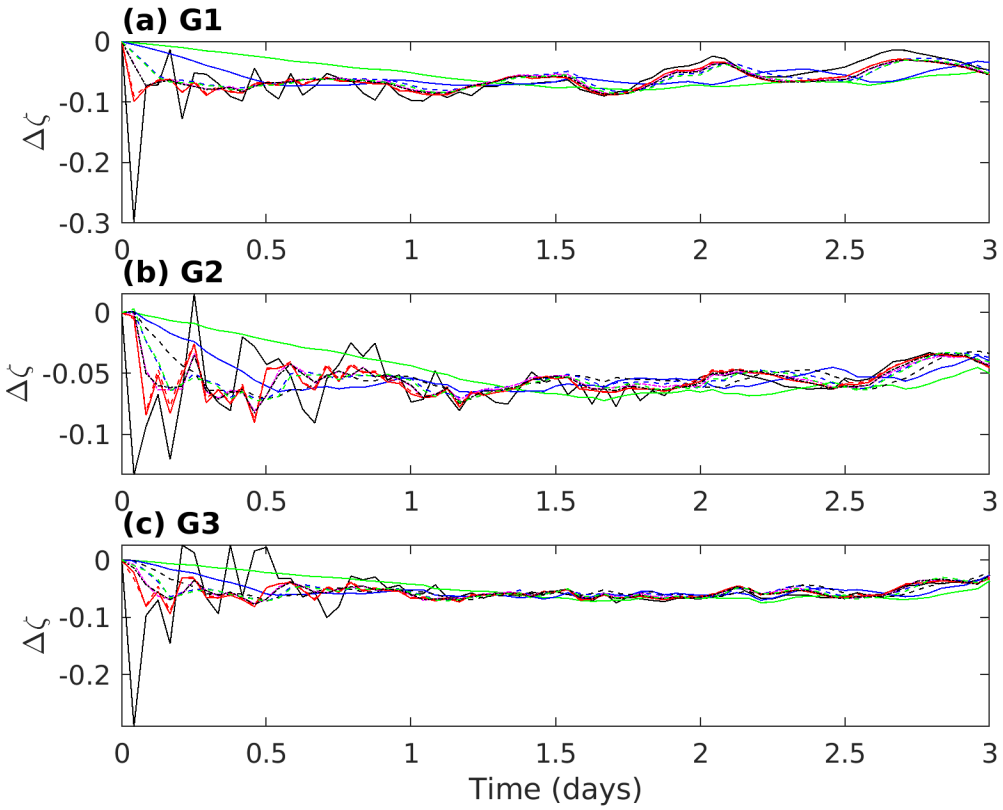

Figure 6: Time series of sea surface elevation *increment* at the locations indicated by the black circle in G2 and G3 and the black triangle in G1 shown in Fig. 4a. *T=0* – black line; *T=1.5* days – green line; *T=0.5* days – blue line; *T=0.25* days – black dashed line; *T=0.125* days – blue dashed line; *T=0.0625* days – magenta dashed-dotted line; *T=0.025* days – red line; IAU on G1 only *T=0.025* days – red dashed line; IAU on G1 only *T=0.0625* days – black dash-dotted line; IAU on G1 only *T=0.125* days – green dashed line.

The gravity wave shock in this example is primarily a result of dynamical imbalances in the 4D-Var analysis on G1. The shock in *all* nested grids can be mitigated by performing IAU only on G1. This is illustrated in Figs. 6 and 7 which also shows the case when the IAU is applied only on G1 over the first 1.5 hours of the 4D-Var window. The fields of sea surface elevation in this case are indistinguishable from those in Figs. 5f and 5i (not shown).

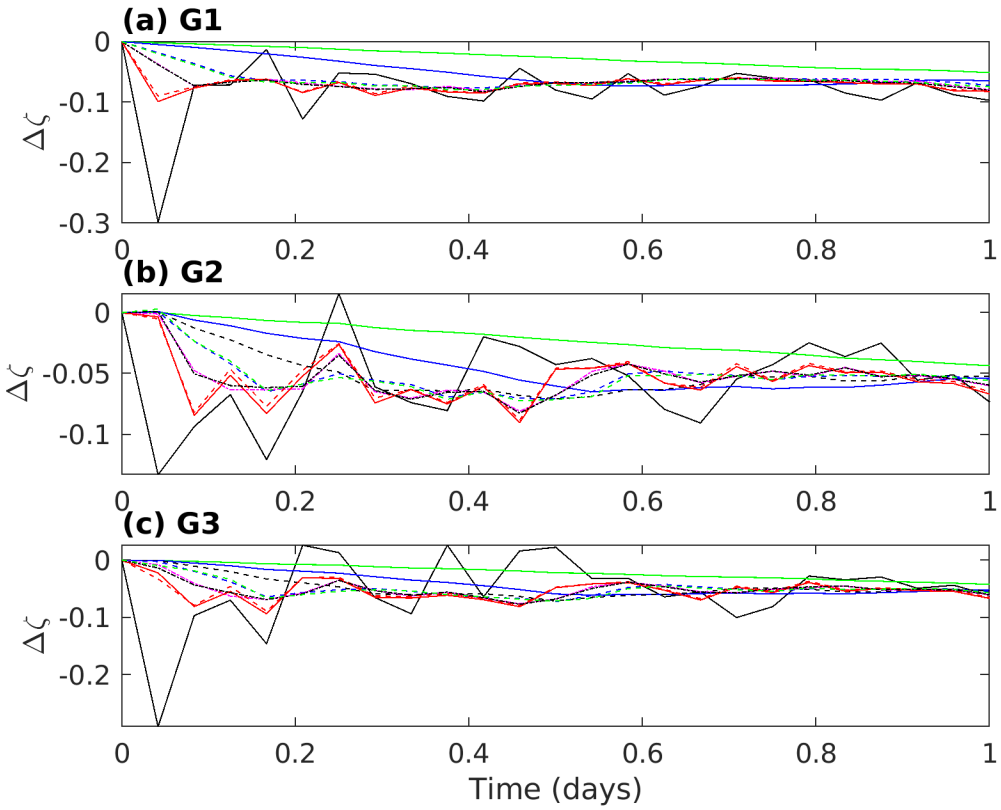

Figure 7: Same as Fig. 6 but showing only the first 24 hours. *T=0* – black line; *T=1.5* days – green line; *T=0.5* days – blue line; *T=0.25* days – black dashed line; *T=0.125* days – blue dashed line; *T=0.0625* days – magenta dashed-dotted line; *T=0.025* days – red line; IAU on G1 only *T=0.025* days – red dashed line; IAU on G1 only *T=0.0625* days – black dash-dotted line; IAU on G1 only *T=0.125* days – green dashed line.

References

Bloom, S.C., L.L. Takacs, A.M. da Silva and D. Ledvina, 1996: Data assimilation using incremental analysis updates. *Mon. Wea. Rev.*, **124**, 1256-1271.

Gauthier, P., and J.-N. Thépaut, 2001: Impact of the digital filter as a weak constraint in the preoperational 4DVAR assimilation system of Météo-France. *Mon. Wea. Rev.*, **129**, 2089–2102.

Machenhaur, B., 1977: On the dynamics of gravity oscillations in a shallow water model with application to non-linear initialization. *Beit. Phys. Atmos.*, **50**, 253-271.

Polavarparu, S., R. Shuzan, A.M. Clayton, D. Sankey and Y. Rochon, 2004: On the relationship between incremental analysis updating and incremental digital filtering. *Mon. Wea. Rev.*, **132**, 2495-2502.